ITERATIVE SOURCE CODED MODULATION: EXIT CHARTS, COMPLEXITY COMPARISONS AND NEW INDEX ASSIGNMENTS

Thorsten Clevorn and Peter Vary

Institute of Communication Systems and Data Processing (ind), RWTH Aachen University, Germany
{clevorn,vary}@ind.rwth-aachen.de

ABSTRACT

Iterative source coded modulation (ISCM) improves the error concealment for source codec parameters without increasing the transmitted bit rate by combining iterative demodulation of higher order modulations and the usage of residual source redundancy in a Turbo process. In this paper we present the enhanced capabilities of ISCM when novel index assignments are applied. A doubling of the previously achievable logarithmic gains [1] is possible. Furthermore, the convergence properties of ISCM are analyzed by EXIT charts and the computational complexity is compared to a rate-1 iterative source-channel decoding (ISCD) system [2]. ISCM exhibits a competitive performance in relation to an equally complex ISCD system.

1. INTRODUCTION

In digital communications codec parameters of encoded speech, audio and video sources exhibits usually considerable residual redundancy in terms of, e.g., non-uniform probability distribution or auto-correlation. Using *error concealment* techniques like *softbit source decoding* (SBSD) [3], *a priori* knowledge on this redundancy can be exploited at the receiver to increase the error robustness. In conjunction with a channel code in [4],[5] the capabilities of SBSD have been enhanced to iterative source-channel decoding (ISCD) by using a Turbo-like decoding algorithm. Even if a rate-1 code is used, significant improvements can be achieved without increasing the bit rate on the channel [2].

In [1] we presented *iterative source coded modulation* (ISCM), which replaces the channel decoder in ISCD by a demodulator for higher order modulations, following the principle of bit-interleaved coded modulation with iterative decoding [6] (BICM-ID). With the demodulator acting as rate-1 code, ISCM enables considerable performance gains compared to non-iterative systems. Possible applications for ISCM are communication systems without channel coding, e.g., DECT.

With novel index assignments according to [7] the capabilities of ISCM can be significantly enhanced further. As shown in this contribution the achievable logarithmic gains by ISCM [1] can be more than doubled. Furthermore, we present an EXIT chart analysis of the convergence behavior of an ISCM system. Finally, a comparison of the computational complexity of ISCM and a respective ISCD system reveals that for systems with approximately similar complexity ISCM exhibits a slightly superior performance.

2. THE ISCM SYSTEM

In this section the design of an ISCM system is very briefly reviewed. For a detailed description we refer to [1]. Fig. 1 depicts the baseband model of the proposed ISCM system. At time instant τ, a source encoder determines a frame $\underline{u}_\tau$ of K_S source codec parameters $u_{\kappa,\tau}$, $\kappa = 1, \ldots K_S$. The rate of source codec parameters $u_{\kappa,\tau}$ is denoted by R_S. Each $u_{\kappa,\tau}$ is quantized to a reproduction level $\bar{u}^{(\xi)}$ with an assigned bit pattern $\mathbf{x}_{\kappa,\tau}$ of M_κ bits. For simplicity we assume $M_\kappa = M$ for all κ. More details on this index assignment are given in Section 3.

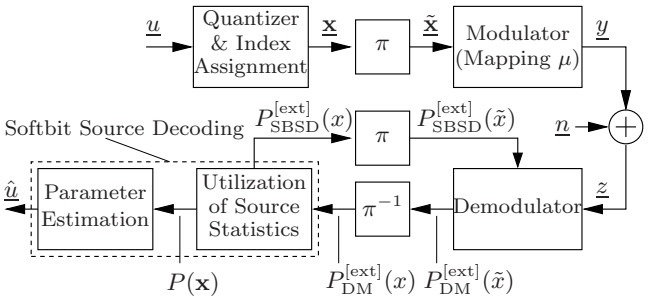

Figure 1: Baseband model of the ISCM system.

The bit-interleaver π permutes the frame $\underline{\mathbf{x}}_\tau$ to $\underline{\tilde{\mathbf{x}}}_\tau$, where $\underline{\tilde{\mathbf{x}}}_\tau$ consists of K_C bit patterns $\tilde{\mathbf{x}}_{k,\tau}$, each with I bits. The modulator maps the interleaved bit patterns $\tilde{\mathbf{x}}_{k,\tau}$ according to a mapping rule μ to complex modulated symbols $y_{k,\tau}$ out of the signal constellation set $\mathcal{Y}$, $y_{k,\tau} = \mu(\tilde{\mathbf{x}}_{k,\tau})$. The modulated symbols are normalized to an average energy of $E\{\|y_{k,\tau}\|^2\} = 1$. The rate of modulated symbols is R_C.

On the channel complex additive white Gaussian noise (AWGN) $n_{k,\tau} = n'_{k,\tau} + \mathrm{j}\, n''_{k,\tau}$ with a known power spectral density of $\sigma_n^2 = N_0$ ($\sigma_{n'}^2 = \sigma_{n''}^2 = N_0/2$) is applied, $z_{k,\tau} = y_{k,\tau} + n_{k,\tau}$. A Rayleigh channel including IQ interleaving is considered in [1].

At the receiver the symbols $z_{k,\tau}$ are evaluated in a Turbo process, which exchanges *extrinsic* probabilities between the demodulator and the softbit source decoder (SBSD). For a detailed description of how to obtain the *extrinsic* probabilities we refer to [6],[1] for the demodulator and to [4],[5],[1] for the SBSD. Finally, the estimated parameter $\hat{u}$ is computed. Note, in all steps at the receiver L-values [8] can be used instead of probabilities P [6],[4].

Beside scrambling the bits for an efficient exchange of *extrinsic* information, the bit-interleaver has a second task. Since the index assignment introduces a different significance for the different bits (see Section 3) and the different bit positions experience an unequal error protection by the higher order modulation (see Section 4), it has to be assured that the most (least) significant bit m_{MSB} (m_{LSB}) is assigned to the most (least) protected bit position i_{MPB} (i_{LPB}) and so on. For $I = M$ and $i_{\mathrm{MPB}}, \ldots i_{\mathrm{LPB}} = 1, \ldots I$ a single reassignment function ψ is sufficient [1],

$$(i_{\mathrm{MPB}}, \ldots i_{\mathrm{LPB}}) = \psi(m_{\mathrm{MSB}}, \ldots m_{\mathrm{LSB}}) \quad . \tag{1}$$

In this case the interleaver π consists of I separate subinterleavers, one for each i, e.g., π_{MSB}, with ψ ensuring the desired assignment of the single bits x and $\tilde{x}$ to these subinterleavers.

3. INDEX ASSIGNMENT

As for *iterative source-channel decoding* (ISCD) the index assignment is also a key parameter for the performance of ISCM [1]. Good index assignments for iterative systems differ significantly from the standard index assignments for the non-iterative case, e.g., Natural Binary (NB).

In [1] we used the SNR optimized (SO) index assignment developed in [9]. Based on simplified constraints like single bit errors the index assignment is optimized in [9] such that the *parameter signal-to-noise ratio* (ParSNR) between the original codec parameter u and its reconstruction $\hat{u}$ is maximized. However, e.g., the parameter correlation is neglected in the optimization process. But this correlation is a key factor, which actually makes substantial gains by iterative source channel decoding possible.

Using EXIT charts [10] a new optimization method is presented in [7]. This method takes the parameter correlation into account and is based on the fact that for perfect *a priori* knowledge the *extrinsic* information obtained by the SBSD can be computed analytically (for details see [7]). The generated EXIT optimized (EO) index assignments show a superior performance compared to the SNR optimized index assignments for ISCD as well as for ISCM. Note, the EO index assignment depends on the auto-correlation ρ, i.e., EO_ρ.

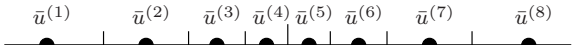

NB	000	001	010	011	100	101	110	111
SO	111	001	010	100	110	101	011	000
$\mathrm{EO}_{0.95}$	110	011	101	000	111	010	100	001

Figure 2: Index Assignments to Quantizer Levels $\bar{u}^{(\xi)}$ for $\rho=0.95$ and $M=3$ bit/parameter: Natural Binary (NB), SNR optimized (SO) [9], and EXIT optimized (EO) [7].

Fig. 2 depicts the index assignments used in this publication. Due to the unequal error protection (UEP) introduced by the higher order modulation an indicator for the significance of the single bits $x^{(m)}$ is required. In [1] we proposed the average (w.r.t. the probability of occurrence $P(\bar{u}^{(\xi)})$) noise energy $\overline{N}_E^{(m)}$ which a single bit error of bit $x^{(m)}$ will generate for a parameter,

$$\overline{N}_E^{(m)} = \sum_{\xi=1}^{2^M} \left(\bar{u}^{(\xi)} - \overline{\bar{u}^{(\xi)}}\right)^2 \cdot P\left(\bar{u}^{(\xi)}\right) \quad . \tag{2}$$

$\overline{\bar{u}^{(\xi)}}$ is the quantizer level with same the assigned bit pattern $\mathbf{x}$, except for an inverted bit $x^{(m)}$. A high $\overline{N}_E^{(m)}$ implies a high significance of bit m. Table 3 shows the values of $\overline{N}_E^{(m)}$ for Lloyd-Max quantization of a Gaussian source ($\sigma_u^2=1$) with $M=3$ bit/parameter. As visible for NB index assignment the bit $m=1$ is by far the most significant bit (MSB) while for SO the bit $m=2$ and for $\mathrm{EO}_{0.95}$ the bit $m=3$ has the highest significance.

Index Assignment	$\overline{N}_E^{(1)}$	$\overline{N}_E^{(2)}$	$\overline{N}_E^{(3)}$
Natural Binary (NB)	5.03	1.51	0.38
SNR optimized [9] (SO)	4.66	5.04	4.66
EXIT optimized [7] ($\mathrm{EO}_{0.95}$)	4.92	4.30	5.03

Table 1: Average Noise Energy $\overline{N}_E^{(m)}$ of a single bit error for a Lloyd-Max quantizer with $M=3$ bit/parameter.

4. MAPPING FOR HIGHER ORDER MODULATION

Based on the performance bound of the bit-error rate (BER) P_b of BICM-ID on Rayleigh fading channels [6] we derived in [1] a measure for the protection level of a bit position i. The derivation assumes error free feedback (EFF), i.e., $P_{\mathrm{SBSD}}^{[\mathrm{ext}]}(\tilde{x}^{(j)}) \in \{0.0, 1.0\}$, for all bits except the considered bit $\tilde{x}^{(i)}$. This results in a BPSK decision for this bit between y and $\check{y}$, where $\check{y}$ possesses the identical bit pattern $\mathbf{x}$ as y except for an inverted bit at position i. The protection level of a bit position i is then given by $\check{d}_h^{2(i)}$, the *harmonic mean* of the squared *Euclidean distances* $\|y-\check{y}\|$ of the possible BPSK decisions for this bit position i, i.e.,

$$\check{d}_h^{2(i)}(\mu) = \left(\frac{1}{2^I} \sum_{b=0}^{1} \sum_{y \in \mathcal{Y}_b^i} \frac{1}{\|y-\check{y}\|^2} \right)^{-1} \quad . \tag{3}$$

The subset $\mathcal{Y}_b^i$ contains all symbols y for which the bit i of the corresponding bit pattern $\mathbf{x}$ is b. The highest $\check{d}_h^{2(i)}$ identifies the most protected bit (MPB), resp. the lowest $\check{d}_h^{2(i)}$ the least protected bit (LPB). For the detailed derivation we refer to [1]. The signal-pair distances $\|y-\check{y}\|$ of the BPSK decisions are depicted on the right side of Fig. 3 for 8PSK-SP (Set-Partitioning) mapping [6]. Similar figures for the other used mappings can be found in [6],[1]. Table 4 lists the $\check{d}_h^{2(i)}$ for these mappings and additionally the *harmonic mean* over all bit positions $\check{d}_h^2$, an indicator asymptotic performance in BICM-ID. The bit pattern assignment of all mappings is arranged such that $i=1$ is the MPB and $i=I$ the LPB. Note, since ISCM reaches a high ParSNR already at relatively low E_b/N_0, the mapping with the highest $\check{d}_h^{2(i)}$ may not perform best, because the constraint of (almost) error free feedback is only fulfilled at higher E_b/N_0.

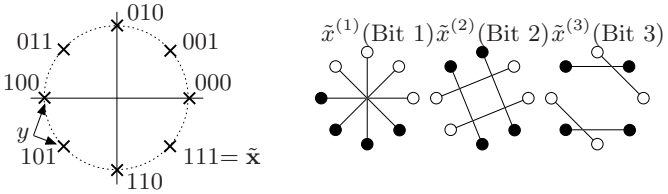

Figure 3: 8PSK-SP mapping with signal-pair distances $\|y-\check{y}\|$ for $\check{d}_h^{2(i)}(\mu)$. $\circ \leftrightarrow \tilde{x}^{(i)}=0$ and $\bullet \leftrightarrow \tilde{x}^{(i)}=1$.

Mapping μ	$\check{d}_h^2$	$\check{d}_h^{2(1)}$	$\check{d}_h^{2(2)}$	$\check{d}_h^{2(3)}$
8PSK-Gray	0.81	1	1	0.59
8PSK-SP (Fig. 3)	1.22	4	2	0.59
8PSK-SSP	2.88	4	3.41	2

Table 2: $\check{d}_h^2$ and $\check{d}_h^{2(i)}$ for different 8PSK mappings.

5. SIMULATION RESULTS

The improved capabilities of ISCM compared to [1] shall be demonstrated by simulation. Instead of using any specific speech, audio, or video encoder, we model $K_S=6$ statistically independent source codec parameters u by a 1^{st} order Gauss-Markov process with auto-correlation $\rho=0.95$, a typical value, e.g., for the scale factors of audio transform codecs. This relatively high auto-correlation helps to illustrate the differences between the different schemes. Each parameter $u_{\kappa,\tau}$ is scalarly quantized by a Lloyd-Max quantizer using $M=3$ bits/parameter. The index assignment is either NB, SO, or $\mathrm{EO}_{0.95}$ with $\psi^{\mathrm{NB}}=(1,2,3)$, $\psi^{\mathrm{SO}}=(2,1,3)$, and $\psi^{\mathrm{EO}}=(3,1,2)$. $I=3$ bits are modulated to one channel symbol. The *parameter signal-to-noise ratio* (ParSNR) between the originally generated parameters $u_{\kappa,\tau}$ and the reconstructed estimates $\hat{u}_{\kappa,\tau}$ is used for quality evaluation. The BER of the bits x is not useful in this context, because the *a priori* information, which is exploited in the SBSD, remains unused for these bits. With $K_S=6$ and $M=3$ the interleaver size is 18 bits. Several simulations showed that such a small interleaver is sufficient for ISCM [1].

The curve marked "○" in Fig. 4 depicts the result of the non-iterative baseline system with NB index assignment, 8PSK-Gray mapping and a single iteration using SBSD. The performance of this baseline system cannot be noticeably improved by iterations. The line "◇" represents results for the ISCM system proposed in [1] with SO index assignment and 8PSK-SSP mapping. A gain close to $\Delta_{E_b/N_0}\approx 1$ dB is achieved in the interesting ParSNR regions. As the curve marked "□" shows, with EO index assignment and 8PSK-SP mapping this gain can be more than doubled, e.g, to $\Delta_{E_b/N_0}>2$ dB at a ParSNR of 14 dB. With these settings almost the performance of a BPSK system ("∗") with a three times higher rate of channel symbols ($R_C^{\mathrm{BPSK}}=3\cdot R_C^{\mathrm{8PSK}}$) is reached. Note, as demonstrated in [1] the gains with ISCM for a Rayleigh fading channel are even larger than for an AWGN channel, e.g., an ISCM 8PSK system actually outperforms a classic BPSK system.

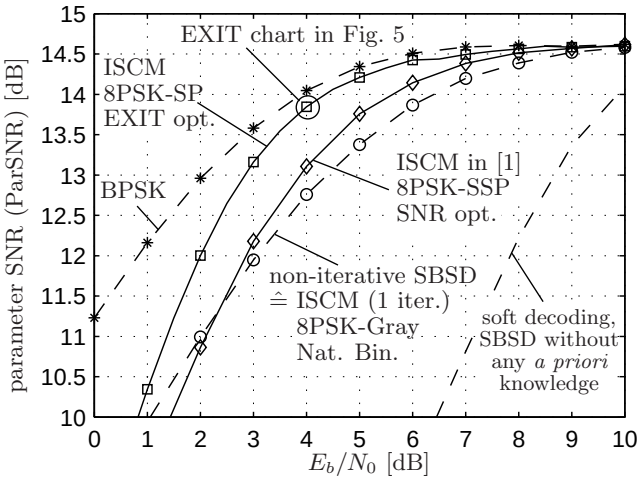

Figure 4: Parameter SNR for 5 iterations, $\rho=0.95$.

6. EXIT CHART ANALYSIS

EXIT (*extrinsic* information transfer) charts [10] are a powerful tool to analyze and optimize the convergence behavior of iterative systems utilizing the Turbo principle, i.e., systems exchanging and refining *extrinsic* information. The capabilities of the components, in our case the demodulator (DM) and the *softbit source decoder* (SBSD), are analyzed separately. The *extrinsic mutual information* $\mathcal{I}^{[\mathrm{ext}]}$ obtained by each component for a certain *a priori mutual information* $\mathcal{I}^{[\mathrm{apri}]}$ is determined. Both, $\mathcal{I}^{[\mathrm{ext}]}$ and $\mathcal{I}^{[\mathrm{apri}]}$, are calculated on the basis of the actual data and the available information, *extrinsic* or *a priori*, for the data. As basis for this calculation usually histograms of the respective L-values, e.g., $L_{\mathrm{DM}}^{[\mathrm{ext}]}$ for $\mathcal{I}_{\mathrm{DM}}^{[\mathrm{ext}]}$, are used. For the EXIT characteristics the *a priori* L-values are simulated as uncorrelated Gaussian distributed, with variance σ_A^2 and mean $\mu_A=\sigma_A^2/2$. In most cases, e.g., for a classical Turbo Code [11], this is a good assumption [10].

Since the *extrinsic* information of one component serves as input *a priori* information for the other component, the two resulting EXIT characteristics are plotted in a single graph with swapped axes. The EXIT characteristic of the demodulator, i.e., of the considered mapping, depends on the E_b/N_0 of the channel. Contrariwise, the EXIT characteristic of the SBSD is independent of the E_b/N_0 since the SBSD has no access to the received channel symbols z. The decoding trajectory (step curve) shows the *mutual information* $\mathcal{I}$ for each iteration in a simulation of the complete system. In the optimization process the components are chosen such that the (first) intersection of their EXIT characteristics moves towards the upper right corner. With the decoding trajectory the number of useful iterations is obtained. Note, the final parameter estimation introduces a dependency between the *mutual information* and the parameter SNR on the used index assignment.

The left side of Fig. 5 depicts the EXIT chart for the curve "□" in Fig. 4 at $E_b/N_0=4$ dB. The mapping is 8PSK-SP and the index assignment is EXIT optimized (EO) with $\psi^{\mathrm{EO}}=(3,1,2)$. As visible the EXIT trajectory reaches the intersection of the EXIT characteristics after approximately 4 or 5 iterations, proving that the 5 iterations in Fig. 4 are sufficient. However, after the first half of the second iteration the decoding trajectory falls significantly short of touching the EXIT characteristic of the demodulator. This behavior does not change for larger block sizes. The histograms of the respective L-values on the right side of Fig. 5 reveal that the assumption of Gaussian distributed L-values made for the EXIT characteristics is not valid anymore for the decoding trajectory. The lower right plot is a histogram on the L-values $L_{\mathrm{SBSD}}^{[\mathrm{ext}]}$ in case the bit x is zero. The histogram for $x=1$ would be flipped on the axis $L=0$. The histogram is not Gaussian, but contains several peaks with different slopes. This agrees with the observation made in [7]. For perfect *a priori* information, i.e., $\mathcal{I}_{\mathrm{SBSD}}^{[\mathrm{apri}]}=1$, the histogram contains only a few discrete peaks and the *extrinsic* information can be determined analytically, enabling the optimization of the index assignment in [7]. The thin lines, depicting the separate histograms for the single bit positions $x^{(m)}$, show that additionally each bit position has a different histogram. The upper right plot shows the histogram of the $L_{\mathrm{DM}}^{[\mathrm{ext}]}$ after the demodulator has used the $L_{\mathrm{SBSD}}^{[\mathrm{ext}]}$ of the lower right plot in the second iteration. The overall histogram is again not Gaussian distributed, providing a possible explanation for the EXIT trajectory not reaching the EXIT characteristic. The histograms of the single bit positions $x^{(i)}$ reveal an approximate but not exact Gaussian distribution of the $L_{\mathrm{SBSD}}^{[\mathrm{ext}]}(x^{(i)})$ as a result of the AWGN channel. In the next iterations the EXIT characteristics are reached always quite close.

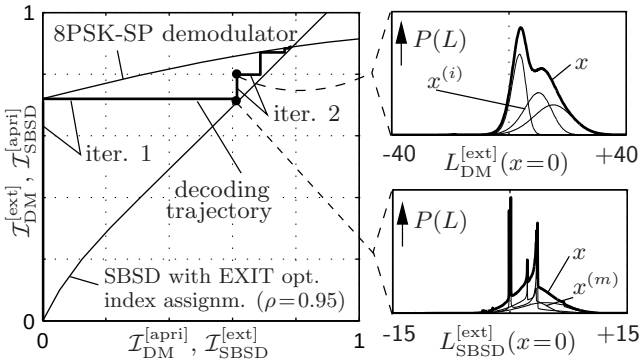

Figure 5: EXIT chart and histograms at $E_b/N_0=4$ dB.

7. COMPLEXITY COMPARISON TO ISCD

In this section we compare the computational complexity of ISCM to the complexity of *Turbo error concealment* by *iterative source-channel decoding* ($\mathrm{ISCD}_{r=1}$) [2]. Using a *recursive non-systematic convolutional* (RNSC) code of rate $r_{\mathrm{RNSC}}=1$ the latter scheme also does not increase the gross bit rate on the channel. The RNSC code replaces the demodulator in the Turbo-loop and provides the *extrinsic* information for the SBSD. Preceding the loop a non-iterative demodulator for higher order modulations can be easily integrated. The

results in [2] show that the performance of $\text{ISCD}_{r=1}$ depends on the code memory J and furthermore that in contrast to ISCM a large interleaver, i.e., a large number of parameters or a significant time-delay, is required.

operation	ISCM in general	$I=3$	$\text{ISCD}_{r=1}$ in general	$J=1$	$J=2$
$+$	2^I-2	6	$3\cdot 2^J-2$	4	10
$*$	$(I-2)\cdot 2^{I-1}+I$	12	$8\cdot 2^J$	16	32

Table 3: Operations per bit x per iteration for ISCM and $\text{ISCD}_{r=1}$ for computing $P_{\text{DM}}^{[\text{ext}]}(x)$ resp. $P_{\text{BCJR}}^{[\text{ext}]}(x)$.

Table 7 lists the number of operations required to obtain the *extrinsic* information for a single bit x for the demodulator in ISCM and the BCJR decoder [12] (with forward, backward and combining cycle) for the RNSC code in $\text{ISCD}_{r=1}$. The values in Table 7 are given for an implementation in the probability domain. However, a transition to L-values [8] would not change the relative complexity. The complexity of the demodulator in ISCM depends on the number of bits I per modulated symbol y, while for $\text{ISCD}_{r=1}$ the code memory J is the parameter. Comparison of the values for the 8PSK modulation for ISCM considered in this paper, i.e., $I=3$, reveal that already an $\text{ISCD}_{r=1}$ system with $J=1$ has a similar (or slightly higher) complexity, stressing the low complexity of ISCM. The other parts of ISCM and $\text{ISCD}_{r=1}$ are identical. In both schemes the conditional probability density $P(z_{k,\tau}|\hat{y})$ needs to be computed once and they use the same SBSD.

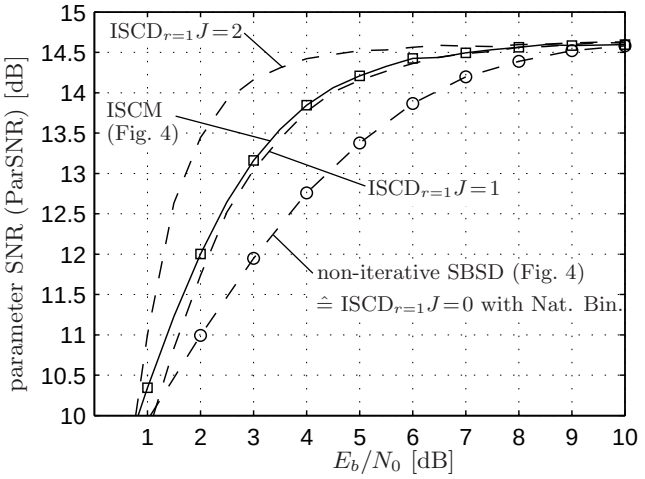

Figure 6: Performance of ISCM and $\text{ISCD}_{r=1}$, $\rho=0.95$, 5 iterations.

In Fig. 6 the parameter SNR performance of ISCM and $\text{ISCD}_{r=1}$ is compared. Similar to Fig. 4 the auto-correlation is set to $\rho=0.95$ and 5 iterations are executed for each system. For ISCM the best curve (marked "□") from Fig. 4 is depicted, which uses 8PSK-SP mapping and EXIT optimized index assignment. The $\text{ISCD}_{r=1}$ schemes employ 8PSK-Gray mapping, the optimum mapping for non-iterative demodulation, and also the EXIT optimized index assignment developed in [7]. As generator polynomials $\mathbf{G}_{\text{RNSC}}^{J}$ for the rate-1 RNSC code with memory J serve $\mathbf{G}_{\text{RNSC}}^{1}=(\frac{1}{1+D})$ and $\mathbf{G}_{\text{RNSC}}^{2}=(\frac{1}{1+D+D^2})$. Note that in [2] computationally much more complex RNSC codes with $J=5$ or $J=6$ were considered for $\text{ISCD}_{r=1}$. An important difference between the ISCM and the $\text{ISCD}_{r=1}$ is the size of the interleaver. ISCM needs only a very small interleaver [1]. In the depicted example a simple 18 bit block interleaver is used, corresponding to 6 parameters per time instant τ. In contrast, $\text{ISCD}_{r=1}$ requires a much larger interleaver. In accordance with [2], we consider 500 parameters per time instant τ, scrambled by a pseudo-random bit-interleaver of size 1500. Thus, in contrast to $\text{ISCD}_{r=1}$, the number of source codec parameters for ISCM is in a realistic range. Additionally, for $\text{ISCD}_{r=1}$ we employ a second pseudo-random bit-interleaver of size $1500+J$ between the demodulator and the BCJR decoder to decorrelate the output of the demodulator. This second interleaver is applied only once per frame, before the iterative process starts. In case the bit pattern of the last modulated symbol y of a frame is not completely filled, the remaining bit positions are zero padded.

Fig. 6 shows that ISCM can slightly outperform the approximately similar complex $\text{ISCD}_{r=1}$ system with $J=1$. By increasing the memory J, and thus increasing exponentially the computational complexity, $\text{ISCD}_{r=1}$ can outperform ISCM. As reference the curve for non-iterative SBSD from Fig. 4 is given. This classic non-iterative approach to *error concealment* can be also regarded as $\text{ISCD}_{r=1}$ with $J=0$ and Natural Binary index assignment.

8. CONCLUSION

In this paper we enhanced the capabilities of *iterative source coded modulation* (ISCM) by novel index assignments. The gains of ISCM compared to conventional non-iterative systems can be more than doubled. Using EXIT charts the convergence behavior and the associated ISCM specific particularities are analyzed. A comparison demonstrates that ISCM can outperform an equally computational complex ISCD system, with the latter one using and requiring a significantly larger interleaver. The possible combination of ISCM and ISCD would result in a Multiple Turbo code.

9. ACKNOWLEDGMENTS

The authors want to thank Marc Adrat for inspiring discussions and Johannes Brauers for the ISCD results in Section 7.

REFERENCES

[1] T. Clevorn, P. Vary, and M. Adrat, "Iterative Source Coded Modulation: Turbo Error Concealment by Iterative Demodulation," *IEEE ICASSP*, Montreal, Canada, May 2004.

[2] M. Adrat and P. Vary, "Iterative Source-Channel Decoding with Code Rates near r=1," *IEEE ICC*, Paris, France, June 2004.

[3] T. Fingscheidt and P. Vary, "Softbit Speech Decoding: A New Approach to Error Concealment," *IEEE Trans. Speech Audio Processing*, pp. 240–251, Mar. 2001.

[4] M. Adrat, P. Vary, and J. Spittka, "Iterative Source-Channel Decoder Using Extrinsic Information from Softbit-Source Decoding," *IEEE ICASSP*, Salt Lake City, Utah, May 2001.

[5] N. Görtz, "On the Iterative Approximation of Optimal Joint Source-Channel Decoding," *IEEE J. Select. Areas Commun.*, pp. 1662–1670, Sept. 2001.

[6] X. Li, A. Chindapol, and J. A. Ritcey, "Bit-Interleaved Coded Modulation With Iterative Decoding and 8PSK Signaling," *IEEE Trans. Comm.*, pp. 1250–1257, Aug. 2002.

[7] M. Adrat and P. Vary, "Iterative Source-Channel Decoding: Improved System Design Using EXIT Charts," *accepted for EURASIP J. on Applied Signal Proc.*, 2005.

[8] J. Hagenauer, E. Offer, and L. Papke, "Iterative Decoding of Binary Convolutional Codes," *IEEE Trans. Comm.*, pp. 429–445, Mar. 1996.

[9] J. Hagenauer and N. Görtz, "The Turbo Principle in Joint Source-Channel Coding," *IEEE ITW 2003*, Paris, France, Mar. 2003.

[10] S. ten Brink, "Convergence Behavior of Iteratively Decoded Parallel Concatenated Codes," *IEEE Trans. Comm.*, pp. 1727–1737, Oct. 2001.

[11] C. Berrou, A. Glavieux, and P. Thitimajshima, "Near Shannon Limit Error-Correcting Coding and Decoding," *IEEE ICC*, Geneva, 1993.

[12] L. R. Bahl, J. Cocke, F. Jelinek, and J. Raviv, "Optimal Decoding of Linear Codes for Minimizing Symbol Error Rate," *IEEE Trans. Inform. Theory*, pp. 284–287, Mar. 1974.